

Enhanced seasonal forecast skill following stratospheric sudden warmings

Article

Accepted Version

Sigmond, M., Scinocca, J. F., Kharin, V. V. and Shepherd, T. G. ORCID: <https://orcid.org/0000-0002-6631-9968> (2013) Enhanced seasonal forecast skill following stratospheric sudden warmings. *Nature Geoscience*, 6 (2). pp. 98-102. ISSN 1752-0908 doi: 10.1038/NGEO1698 Available at <https://centaur.reading.ac.uk/30624/>

It is advisable to refer to the publisher's version if you intend to cite from the work. See [Guidance on citing](#).

To link to this article DOI: <http://dx.doi.org/10.1038/NGEO1698>

Publisher: Nature Publishing

All outputs in CentAUR are protected by Intellectual Property Rights law, including copyright law. Copyright and IPR is retained by the creators or other copyright holders. Terms and conditions for use of this material are defined in the [End User Agreement](#).

www.reading.ac.uk/centaur

CentAUR

Central Archive at the University of Reading

Reading's research outputs online

Enhanced seasonal forecast skill following stratospheric sudden warmings

M. Sigmond^{1*}, J. F. Scinocca², V. V. Kharin², T. G. Shepherd^{1,3}

¹Department of Physics, University of Toronto, Toronto, Ontario, Canada.

²Canadian Centre for Climate Modelling and Analysis, Environment Canada, Victoria, British Columbia, Canada

³Department of Meteorology, University of Reading, Reading, United Kingdom.

* E-mail: sigmond@atmosph.physics.utoronto.ca

Submitted to Nature Geoscience, July 2012 – Revised October 2012

Advances in the field of seasonal forecasting have brought widespread socio-economic benefits. However, seasonal forecast skill in the extratropics is relatively modest¹, which has prompted the seasonal forecasting community to search for additional sources of predictability^{2,3}. For over a decade it has been suggested that the stratosphere can act as a source of enhanced seasonal predictability, as long-lived circulation anomalies in the lower stratosphere following Stratospheric Sudden Warmings are associated with same-signed circulation anomalies in the troposphere for up to two months^{4,5}. Here we show that such enhanced predictability can be realized in a dynamical seasonal forecast system, thus opening the door to prediction of a comprehensive suite of parameters of socio-economic relevance. We employ a dynamical forecast system with a good representation of the stratosphere to perform ensemble model forecasts initialized at the onset date of Stratospheric Sudden Warmings. Our model forecasts faithfully reproduce the observed mean tropospheric response in the following months, with enhanced forecast skill of atmospheric circulation patterns, surface temperature over Northern Russia and Eastern Canada, and North Atlantic precipitation. Our results imply that seasonal forecast systems are likely to produce significantly higher forecast skill for certain regions when initialized during Stratospheric Sudden Warmings.

Skillful seasonal forecasts rely on the predictability of slowly-varying components of the climate system, such as sea surface temperature (SST), sea ice, snow, and soil moisture. Most of the skill that is currently obtained by seasonal forecast systems stems from the predictability of El Niño Southern Oscillation (ENSO) and its remote influences¹. In general, ENSO's influence declines

with increasing distance from the tropical Pacific Ocean, resulting in relatively smaller forecast skill for the extratropics, especially over Northern Eurasia^{1,2}. However, two recent reports^{2,3} have suggested that the maximum seasonal forecast skill has not been achieved, and have identified the stratosphere as an untapped source of enhanced seasonal predictability. This is based on the observation that rapid breakdowns of the westerly flow (or polar vortex) in the polar winter stratosphere (known as Stratospheric Sudden Warmings or SSWs) tend to be followed by a tropospheric circulation pattern that is often described as the negative phase of the Northern Annular Mode (NAM)⁴, with a corresponding signature in surface temperature that is complementary to that of ENSO (i.e. strongest over the Atlantic sector and Northern Eurasia, where the ENSO impact is modest)⁵. However, SSWs are highly nonlinear events that are only predictable a week or two in advance^{6,7}. Consequently, the enhanced seasonal predictability coming from the stratosphere is likely to be conditional (i.e., only after a SSW has occurred).

Previous studies of enhanced seasonal predictability associated with SSWs are mainly based on simple statistical models⁸⁻¹¹. Seasonal forecast systems based on dynamical models are able to capture the average tropospheric state following SSWs to some extent¹², but it is not evident that this is associated with a detectable increase in forecast skill of surface weather¹³. Here we demonstrate that a dynamical forecast system initialized at the time of a SSW is able to predict the mean tropospheric circulation response in the following months. We also show that the forecast skill of socio-economically relevant variables such as surface temperature and precipitation is significantly enhanced relative to the forecast skill in a set of unconditional forecasts (i.e. control forecasts that are not explicitly initialized during SSWs).

62

63 The dynamical forecast system in this study employs the Canadian Middle Atmosphere Model
64 (CMAM)¹⁴. Retrospective forecasts (also known as hindcasts) are initialized at 20 SSW dates
65 between 1970 and 2009 (hereafter referred to as the SSW forecasts), each consisting of 10
66 ensemble members. In all model forecasts, SST anomalies that occur at initialization time are
67 thereafter relaxed to climatology as described in the Methods section. This allows us to exclude
68 predictability that may arise from SSTs (e.g., related to the ENSO phenomenon), thus isolating
69 predictability that stems from atmospheric and associated land initializations. We focus on the
70 ensemble mean forecast averaged over the 16-60 days after the SSWs. Forecast anomalies are
71 defined as differences relative to the climatology of the unforced (freely running) model (see the
72 Methods section).

73

74 The model prediction of the anomalous tropospheric state following SSWs agrees very well with
75 observations (Fig. 1; see also Supplementary Fig. S1). Figs. 1a and 1c (contours) show that
76 averaged over all 20 SSW cases, the observed Sea Level Pressure (SLP) pattern is characterized
77 by a dipole with anomalously high SLP at high latitudes and anomalously low SLP at mid-
78 latitudes. This pattern is often described as a negative NAM pattern. It is well reproduced by the
79 model (Figs. 1b and 1d), except that the centre of anomalously low SLP in the North Atlantic is
80 shifted east relative to that in the observations. The negative NAM pattern is associated with a
81 near-surface easterly wind anomaly at NH mid-latitudes (not shown), which results in increased
82 (decreased) advection of relatively warm ocean air to Eastern Canada (Northern Russia)¹⁵. The
83 resulting warm anomaly over Eastern Canada and cold anomaly over Northern Russia (Fig. 1a)

is again well captured by the model (Fig. 1b). The negative NAM pattern is also consistent with an equatorward shift of the storm track (not shown), which is associated with decreased precipitation (PCP) over the high-latitude Atlantic, and increased PCP over the mid-latitude Atlantic (Fig. 1c). This feature is again well reproduced by the model (Fig. 1d), except that, consistent with the SLP, the centre of anomalously high PCP in the mid-latitude North Atlantic is shifted east relative to that in the observations.

The implications for forecast skill can be understood by considering Fig. 2a. It shows a scatter plot of the observed versus forecast NAM index at 1000 hPa, where each point represents one (ensemble mean) model forecast initialized at a particular SSW date. Most points are located in the lower left quadrant, reflecting the fact that on average both the observed and modeled surface NAM following the SSWs is negative. The average horizontal location (represented by the vertical dashed line) is the mean observed value (-0.44). The horizontal error bar shows that the observed mean surface NAM response is statistically significant at the 95% confidence level. The average modeled surface NAM, which is the average vertical location of the points, is somewhat larger (-0.74) and also statistically significant. The correlation between observed and modeled surface NAM (hereafter referred to as the Correlation Skill Score (CSS) or simply ‘forecast skill’) is substantial ($r=0.55$) and statistically significant at the 99% confidence level (see also Fig. 4a), which is a reflection of the tendency of the points in the scatter plot to be shifted towards the lower left quadrant. Thus, we find that our model has a significant skill in forecasting the surface circulation for a lead time of 16-60 days.

Some of the skill in the SSW forecasts may, in principle, also stem from predictability of slowly varying boundary conditions such as soil moisture (as noted above, the model forecasts are designed to exclude SST effects on predictability). To quantify such skill, we performed a control set of forecasts initialized at the same calendar dates as the SSWs, but in the year preceding and the year following the SSWs. The results are plotted in Fig. 2b. We find a similar spread in the observed and modeled surface NAM index as in the SSW forecasts, but instead of being shifted towards a particular quadrant, the cloud of points is centered near the origin. The near-zero (-0.01) CSS for the surface NAM demonstrates that the unconditional control forecasts do not contain any forecast skill for the surface circulation for a lead time of 16-60 days, demonstrating that the skill in the SSW forecasts does come from the SSWs themselves. Note that the similar spread in the cloud of points in Figures 2a and 2b suggests that the inherent predictability of the surface NAM is not enhanced after SSWs, but instead that the increased correlation skill score in the SSW forecasts is largely due to the shift in the mean NAM towards negative values.

The vertical profile of the mean NAM index following the SSWs is well captured by the model forecasts (Fig. 3a). The model slightly overestimates the mean NAM response near the surface, but correctly captures the vertical structure which maximizes in the lower stratosphere and exhibits a minimum in the middle troposphere. The corresponding forecast skill is shown in Fig. 3b. Consistent with Fig. 2, it shows that near the surface the forecast skill is substantial and significant for the SSW forecasts, and near-zero and not significant for the control forecasts. Except for the mid to upper troposphere, forecast skill of the NAM following SSWs is

substantial, statistically significant, and significantly larger than in forecasts that are not constrained to be initialized during SSWs.

The influence of SSWs on forecast skill for the NAM index and for Northern Hemisphere surface variables is summarized in Fig. 4. The statistical significance of the difference between the CSS in the SSW and control forecasts is labeled by p-values in this figure, which represent the confidence level at which enhanced forecast skill can be associated with SSWs and which are determined by bootstrapping. This level exceeds 99% ($p < 0.01$) for the NAM at 100 and 1000 hPa (Fig. 4a), and is 98% for the North Atlantic Oscillation (NAO) (which is the local Atlantic manifestation of the surface NAM and is defined here as the SLP difference between Iceland and the Azores) (Fig. 4b). For SLP, Surface Temperature (ST) and PCP, forecast skill averaged over 20-90°N (left bars in Figs. 4b-d) is statistically significant in the SSW forecasts, and enhanced relative to that in the control forecasts. However, this enhancement is only statistically significant for SLP ($p = 0.04$). Focusing on localized regions, significant skill enhancement can be detected for ST in Northern Russia and Eastern Canada (Fig. 4c) and for the PCP gradient over the Northern Atlantic (Fig. 4d).

For more than a decade it has been suggested that the stratosphere can act as a source of seasonal predictability. The results in this paper confirm that such predictability can be realized in dynamical forecast systems. A requirement for the predictability to be realized is a model that realistically simulates the tropospheric response to SSWs. Even though current seasonal forecast

systems (which generally have a poorly represented stratosphere) capture this response with some credibility¹², it has been suggested that the response is more realistic in models with a well-represented stratosphere¹⁶ such as the model employed here. Also, as SSWs themselves are better predicted with a longer lead time in such models⁷ it may be possible to elevate seasonal forecast skill by raising the model lid and increasing vertical resolution in the stratosphere^{2,17}.

In assessing the practical implications of these results it must be noted that the enhanced predictability is highly conditional and contingent upon the occurrence of SSWs, which occur on average in six out of ten winters. Although the seasonal predictability associated with ENSO is also conditional, there are two important differences: 1) SSWs are inherently less predictable than ENSO giving a shorter lead time for the opportunity, and 2) the window of opportunity is comparatively limited as the SSW influence on the troposphere only lasts for about half to two-thirds of a season. Therefore the potential enhancement of forecast skill associated with SSWs is likely to be very limited in standard seasonal forecasts which are generally issued once a month. In an attempt to exploit this source of predictability stemming from the stratosphere, seasonal forecast centers could issue special forecasts once a SSW has been identified in observations. This would require additional computational resources as forecast simulations initialized at non-standard dates would have to be performed. The results presented here suggest that such additional computational effort would be well justified, as the special forecasts are likely to feature enhanced forecast skill with potentially widespread socio-economic benefits.

Methods

Observational dataset and model forecasts

The 1970-1988 data from ERA-40 (ref. 18) and the 1989-2009 data from ERA-Interim¹⁹ are merged to provide an observational dataset that is used to initialize and verify the model. To identify Stratospheric Sudden Warmings (SSWs), we apply a criterion based on the Northern Annular Mode (NAM) index instead of the standard WMO criterion which is based on the zonal-mean zonal wind at 10 hPa and 60°N, as the NAM index has been shown to better gauge stratosphere-troposphere coupling than zonal-mean zonal wind²⁰. A SSW is defined to occur when the NAM index calculated from year-round daily zonal-mean geopotential height following ref. 20 first drops below -2.5 at 30 hPa. For winters with multiple SSWs, we only consider the warming with the largest amplitude. Following this procedure 20 warming cases are found between November 1970 and March 2009.

The dynamical seasonal forecast system is based on the Canadian Middle Atmosphere Model (CMAM)¹⁴, which has 71 vertical levels from the surface up to about 100 km at T63 horizontal resolution. To assess the forecast skill following SSWs we performed 10-member ensemble model forecasts initialized at the 20 SSW dates identified from the observations. The 10 initial states for each SSW are obtained as follows. Ten model runs are started from 10 slightly different atmospheric states on January 1, 1970. In these ‘assimilation’ runs, the spatial scales of the vorticity, divergence and temperature that can be represented by spectral truncation T21 are relaxed towards the time-evolving reanalyses between 1970 and 2009. The relaxation time is 24 hours, which is selected such that the simulated state closely follows the observed one, and the

resulting RMS spread between ensemble members roughly matches the RMS spread between the different reanalysis data sets. The initial atmospheric and land conditions used for the model forecasts at the onset date of the observed SSWs are obtained from these 10 assimilation runs. The initial sea surface temperature (SST) and sea-ice fields are taken from the HadISST dataset²¹. Instead of persisting the SST anomaly that occurs at initialization time for the duration of the model forecast, which is common for operational two-tier seasonal forecasts, we linearly relax the SST anomaly towards climatology in the first 2 weeks of the forecasts. We apply this procedure to exclude predictability that may arise from SSTs, thus isolating the predictability that stems directly from atmospheric perturbations (i.e., SSWs) alone.

To assess if the skill for the forecasts initialized during SSWs is significantly larger than a typical, unconditional forecast, we performed a control set of forecasts initialized at the same calendar dates as the SSWs, but in the year preceding and the year following the SSWs. For the warming that occurred in the 1970-1971 (2008-2009) winter, the control forecast in only the following (previous) winter is performed, as no initial conditions were available for the 1969-1970 (2009-2010) winters. This results in 38 control forecasts, which are compared to the 20 SSW forecasts.

In order to calculate anomalies of meteorological fields in the forecast runs, a reference model climatology must be defined. For this purpose, we performed 10-member ensemble model simulations for the period 1970-2009 with prescribed HadISST SST and sea-ice fields, referred to as AMIP runs. Anomalies of sea level pressure (SLP), Surface Temperature (ST) and Precipitation (PCP) in the model forecasts are calculated relative to the corresponding ensemble

mean climatologies in these AMIP runs. The daily NAM index in the model forecasts is obtained by projecting zonal mean geopotential height anomalies relative to the corresponding AMIP climatology onto the observed NAM pattern. We note that during the first ~15 days of the forecasts the model drifts from observations to the mean behaviour of the AMIP runs (see Supplementary Material). Therefore our analysis focusses on days 16-60 after the SSWs.

Forecast skill quantification

The forecast skill is quantified by the Correlation Skill Score (CSS) defined as follows. Let F_m represent the ensemble mean forecast of a variable (e.g., ST) averaged over a certain period (in this paper, days 16-60) after the forecast initialization date indexed by $m = 1, \dots, M$, and X_m represent the corresponding observed value. $M = 20(38)$ for the SSW (control) forecasts.

The CSS is given by:

$$CSS = \frac{Cov_{X,F}}{\sqrt{Var_X Var_F}},$$

where

$$Cov_{X,F} = \frac{1}{M} \sum_{m=1}^M X'_m F'_m,$$

$$Var_X = \frac{1}{M} \sum_{m=1}^M X'^2_m,$$

$$Var_F = \frac{1}{M} \sum_{m=1}^M F'^2_m.$$

For SLP, ST, and PCP, X'_m is the observed anomaly relative to the 1970-2009 observed climatology, and F'_m is the model forecast anomaly relative to the climatology in the AMIP runs. For the NAM index, X'_m and F'_m represent the values of the observed and forecast NAM index itself since it is already calculated from anomalies of geopotential height. Statistical significance

of the CSS is determined in a bootstrapping procedure by random sampling with replacement of M pairs of F'_m and X'_m .

References

1. Oldenborgh, G.J. van, Balmaseda, M., Ferranti, L., Stockdale, T.N. & Anderson, D.L.T. Evaluation of atmospheric fields from the ECMWF seasonal forecasts over a 15-year period. *J. Clim.* **18**, 3250-3269 (2005).
2. Kirtman, B. & Pirani, A. WCRP position paper on seasonal prediction. *WCRP Informal Report* **3**, (2008).
3. NRC, *Assessment of Intraseasonal to Interannual Climate Prediction and Predictability* (National Academies Press, 2010).
4. Baldwin, M.P. & Dunkerton, T.J. Stratospheric harbingers of anomalous weather regimes. *Science* **294**, 581-4 (2001).
5. Thompson, D.W.J., Baldwin, M.P. & Wallace, J.M. Stratospheric Connection to Northern Hemisphere Wintertime Weather: Implications for Prediction. *J. Clim.* **15**, 1421-1428 (2002).
6. Gerber, E.P., Orbe, C. & Polvani, L.M. Stratospheric influence on the tropospheric circulation revealed by idealized ensemble forecasts. *Geophys. Res. Lett.* **36**, L24801 (2009).

- 255 7. Marshall, A.G. & Scaife, A.A. Improved predictability of stratospheric sudden warming
256 events in an atmospheric general circulation model with enhanced stratospheric
257 resolution. *J. Geophys. Res.* **115**, D16114 (2010).
- 258 8. Baldwin, M.P. *et al.* Stratospheric memory and skill of extended-range weather forecasts.
259 *Science* **301**, 636-40 (2003).
- 260 9. Charlton, A.J., O'Neill, A., Stephenson, D.B., Lahoz, W.A. & Baldwin, M.P. Can
261 knowledge of the state of the stratosphere be used to improve statistical forecasts of the
262 troposphere? *Q. J. R. Meteorol. Soc.* **129**, 3205-3224 (2003).
- 263 10. Christiansen, B. Downward propagation and statistical forecast of the near-surface
264 weather. *J. Geophys. Res.* **110**, D14104 (2005).
- 265 11. Siegmund, P. Stratospheric polar cap mean height and temperature as extended-range
266 weather predictors. *Mon. Weather Rev.* **133**, 2436-2448 (2005).
- 267 12. Maycock, A.C., Keeley, S.P.E., Charlton-Perez, A.J. & Doblas-Reyes, F.J. Stratospheric
268 circulation in seasonal forecasting models: implications for seasonal prediction. *Clim.*
269 *Dyn.* **36**, 309-321 (2011).
- 270 13. Mukougawa, H., Hirooka, T. & Kuroda, Y. Influence of stratospheric circulation on the
271 predictability of the tropospheric Northern Annular Mode. *Geophys. Res. Lett.* **36**,
272 L08814 (2009).
- 273 14. Scinocca, J.F., McFarlane, N. A., Lazare, M., Li, J. & Plummer, D. Technical Note: The
274 CCCma third generation AGCM and its extension into the middle atmosphere. *Atmos.*
275 *Chem. Phys.* **8**, 7055-7074 (2008).

15. Thompson, D.W. & Wallace, J.M. Regional climate impacts of the Northern Hemisphere annular mode. *Science* **293**, 85-9 (2001).
16. Hardiman, S.C., Butchart, N., Hinton, T.J., Osprey, S.M. & Gray, L.J. The effect of a well resolved stratosphere on surface climate: Differences between CMIP5 simulations with high and low top versions of the Met Office climate model. *J. Clim.*, **25**, 7083–7099 (2012).
17. Roff, G., Thompson, D.W.J. & Hendon, H. Does increasing model stratospheric resolution improve extended-range forecast skill? *Geophys. Res. Lett.* **38**, L05809 (2011).
18. Uppala, S.M. *et al.* The ERA-40 re-analysis. *Q. J. R. Meteorol. Soc.* **131**, 2961-3012 (2005).
19. Dee, D.P. *et al.* The ERA-Interim reanalysis: configuration and performance of the data assimilation system. *Q. J. R. Meteorol. Soc.* **137**, 553-597 (2011).
20. Baldwin, M.P. & Thompson, D.W.J. A critical comparison of stratosphere–troposphere coupling indices. *Q. J. R. Meteorol. Soc.* **135**, 1661–1672 (2009).
21. Rayner, N. A. *et al.* Global analyses of sea surface temperature, sea ice, and night marine air temperature since the late nineteenth century. *J. Geophys. Res.* **108**, (D14), 4407 (2003).

Figure 1 | Surface climate response to SSWs. a-d, Mean anomaly averaged over days 16-60 after all SSWs of sea level pressure (contours), surface temperature (shading in **a** and **b**) and precipitation (shading in **c** and **d**) for the observations (**a** and **c**) and the model forecasts (**b** and **d**). Contour interval for sea level pressure is 1 hPa (... , -1.5, -0.5, 0.5,...), and solid (dashed) contours denote positive (negative) values. Black dots represent statistical significance at the 90% confidence level (determined by bootstrapping) of the shaded quantities. Observed (modeled) SLP anomalies are generally significant at the 90% level where the mean anomaly exceeds ~1.5 (0.5) hPa.

Figure 2 | Observed versus forecast 1000 hPa NAM index. a-b, Scatter plot of the observed versus forecast NAM index at 1000 hPa averaged over 16-60 days following the 20 SSWs (**a**) and the 38 control dates (**b**). The vertical dashed line and corresponding black dot represent the average observed value, and the horizontal error bar and corresponding gray shading its 95% confidence interval (as determined by bootstrapping). The horizontal dashed line and corresponding black dot represent the average forecast value, and the vertical error bar and corresponding gray shading its 95% confidence interval.

Figure 3 | Vertical profile of the mean NAM and of the CSS of the NAM. a-b The mean NAM index averaged over 16-60 days after all SSWs (red) and the control dates (blue) as a function of height for the observations (thick line) and the model forecasts (thin line) **(a)**. The error bars represent the 95% confidence interval for the model forecast. The forecast skill as quantified by the CSS as a function of height **(b)**. The difference between the SSW and control CSS is statistically significant at the 95% level where the error bars do not overlap.

Figure 4 | The CSS of various variables. a-d, The CSS of the NAM at 100 and 1000 hPa **(a)**, NAO index **(b)**, surface temperature (ST) over Northern Russia and Eastern Canada (indicated by the blue boxes in Figs. 1a and 1b) **(c)**, precipitation (PCP) difference between the high latitude and mid-latitude Northern Atlantic (indicated by the blue boxes in Figs. 1c and 1d) **(d)**, and the CSS averaged over 20-90°N for SLP **(b)**, ST (land only) **(c)** and PCP **(d)**. Red (blue) bars represent the SSW (control) forecasts for a forecast range of 16-60 days. The thin lines represent the 95% confidence interval. P-values for the difference between the SSW and control CSS are given. This difference is statistically significant at the 95% level when the thick brown lines do not overlap.

336 **Correspondence**

337 Correspondence and requests for materials should be addressed to M.S. (email:

338 sigmond@atmosp.physics.utoronto.ca)

339 **Acknowledgments**

340 Michael Sigmond gratefully acknowledges funding by Environment Canada through a Grants

341 and Contributions Agreement with the University of Toronto. We thank Bill Merryfield, John

342 Fyfe and Nathan Gillett for their helpful comments.

343 **Author contributions**

344 M.S., J.F.S. and V.V.K. designed the experiments. All authors interpreted the results and

345 contributed to writing the paper.

346 **Additional Information**

347 Supplementary information accompanies this paper on www.nature.com/naturegeoscience.

348 **Competing financial interests**

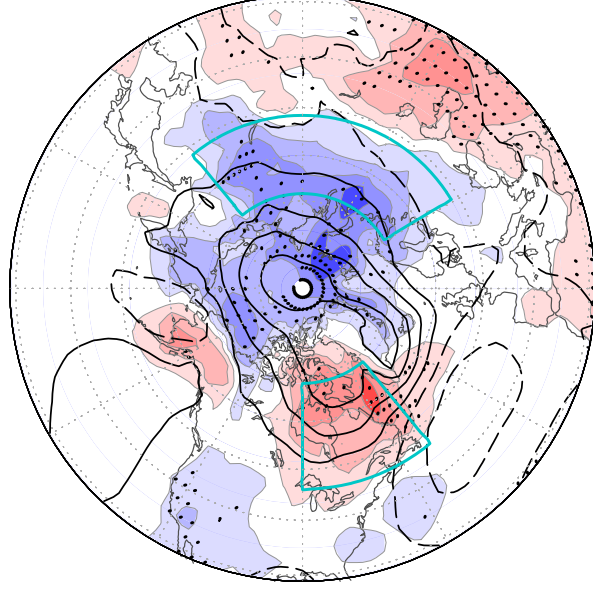
349 The authors declare no competing financial interests.

350

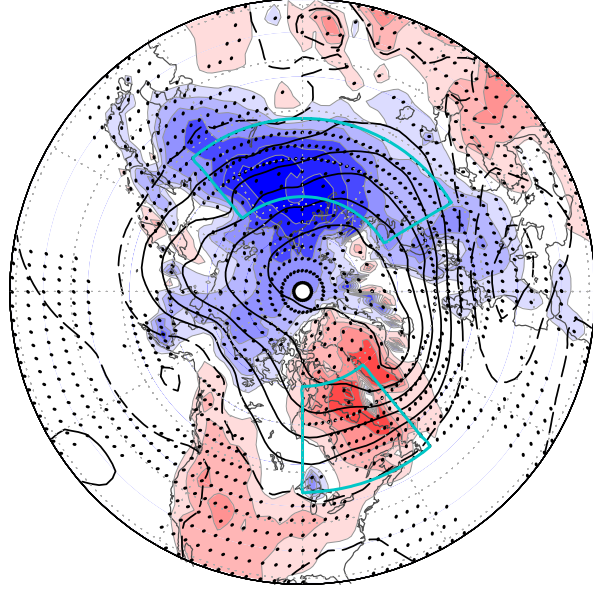
351

352

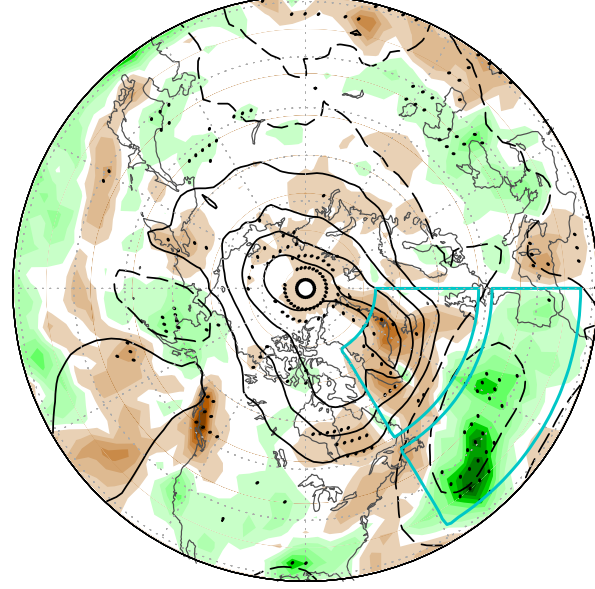
a SLP and ST (Observations)



b SLP and ST (Forecast)



c SLP and PCP (Observations)



d SLP and PCP (Forecast)

